Identification of Novel Purine and Pyrimidine Cyclin-Dependent Kinase Inhibitors with Distinct Molecular Interactions and Tumor Cell Growth Inhibition Profiles

Christine E. Arris,[#] F. Thomas Boyle,[§] A. Hilary Calvert,[#] Nicola J. Curtin,[#] Jane A. Endicott,[¶] Elspeth F. Garman,[¶] Ashleigh E. Gibson,[#] Bernard T. Golding,[#] Sharon Grant,[#] Roger J. Griffin,[#] Philip Jewsbury,[§] Louise N. Johnson,[¶] Alison M. Lawrie,[¶] David R. Newell,*[,#] Martin E. M. Noble,[¶] Edward A. Sausville,[⊥] Robert Schultz,[⊥] and Wyatt Yu[¶]

Cancer Research Unit and Department of Chemistry, University of Newcastle, Newcastle upon Tyne, NE2 4HH U.K., AstraZeneca Pharmaceuticals, Alderley Park, Cheshire, U.K., Laboratory of Molecular Biophysics and Department of Biochemistry, University of Oxford, Oxford, OX1 3QU U.K., and Developmental Therapeutics Program, National Cancer Institute, Bethesda, Maryland 20892-7458

Received December 23, 1999

Substituted guanines and pyrimidines were tested as inhibitors of cyclin B1/CDK1 and cyclin A3/CDK2 and soaked into crystals of monomeric CDK2. O^6-Cyclohexylmethylguanine (NU2058) was a competitive inhibitor of CDK1 and CDK2 with respect to ATP (K_i values: CDK1, 5 ± 1 μM; CDK2, 12 ± 3 μM) and formed a triplet of hydrogen bonds (i.e., NH-9 to Glu 81, N-3 to Leu 83, and 2-NH_2 to Leu 83). The triplet of hydrogen bonding and CDK inhibition was reproduced by 2,6-diamino-4-cyclohexylmethyloxy-5-nitrosopyrimidine (NU6027, K_i values: CDK1, 2.5 ± 0.4 μM; CDK2, 1.3 ± 0.2 μM). Against human tumor cells, NU2058 and NU6027 were growth inhibitory in vitro (mean GI_{50} values of 13 ± 7 μM and 10 ± 6 μM, respectively), with a pattern of sensitivity distinct from flavopiridol and olomoucine. These CDK inhibition and chemosensitivity data indicate that the distinct mode of binding of NU2058 and NU6027 has direct consequences for enzyme and cell growth inhibition.

Introduction

The cyclin-dependent kinases (CDKs) are a family of serine-threonine protein kinases which control cell cycle progression in proliferating eukaryotic cells.[1−5] The activity of CDKs is dependent upon the presence of cyclin partners whose levels are sequentially regulated to ensure that the phases of the cell cycle proceed in the correct order. For example, cyclins of the D family complex with CDKs 4 and 6 during G1 phase, cyclin E with CDK2 in late G1, cyclin A with CDK2 in S phase, and cyclin B with CDK1 (also known as cdc2) in late G2/M. Aberrant CDK control and consequent loss of cell cycle checkpoint function have been directly linked to the molecular pathology of cancer.[6] For example, cyclin overexpression (e.g., cyclin D), loss of function of endogenous CDK inhibitors (e.g., p16 deletion or p21 loss secondary to p53 defects), and CDK substrate alterations (e.g., retinoblastoma gene mutations) have been widely documented in human tumors.[6] These CDK-related events are among the most common genetic changes found in human tumors and, clinically, they often confer a poor prognosis.

In view of the strong link between CDKs and the molecular pathology of cancer, CDKs are being investigated as possible targets for therapeutic intervention.[7−9]

Chart 1. Chemical Structures of CDK Inhibitors

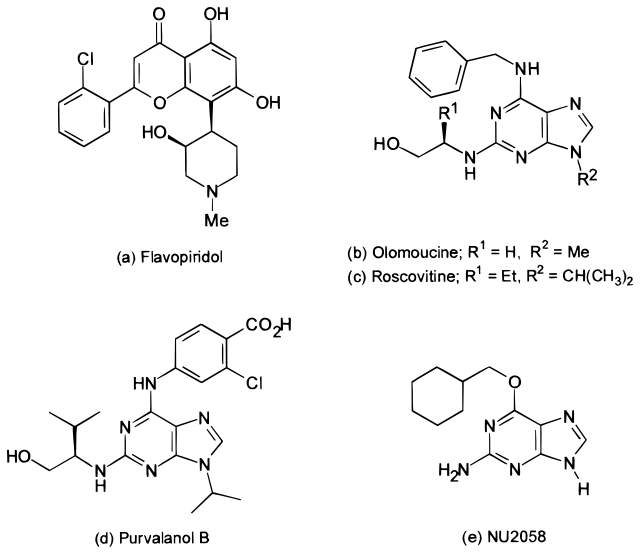

CDK inhibitors should function as non-DNA-interactive antiproliferative agents, thereby avoiding treatment-induced DNA damage in normal tissues and the consequent carcinogenic risk. Furthermore, when used in combination with cytotoxic drugs, reestablishing an otherwise deficient cell cycle checkpoint may enhance the activity of conventional treatments. Studies with first-generation CDK inhibitors support a role for the use of these agents as both single agents and in combination with cytotoxic drugs (see below).

A lead CDK inhibitor is flavopiridol (Chart 1a) which has recently completed Phase I clinical evaluation.[10] Evidence of activity was seen in the Phase I trial of

* Address correspondence to this author at the Cancer Research Unit, Medical School, University of Newcastle, Framlington Place, Newcastle NE2 4HH, England, U.K. E-mail: herbie.newell@ncl.ac.uk. Telephone: -44-191-222-8057. Fax: -44-191-222-7556.
[#] Cancer Research Unit and Department of Chemistry, University of Newcastle.
[§] AstraZeneca Pharmaceuticals.
[¶] Laboratory of Molecular Biophysics and Department of Biochemistry, University of Oxford.
[⊥] Developmental Therapeutics Program, National Cancer Institute.

10.1021/jm990628o CCC: $19.00
Published on Web 07/11/2000

Chart 2. Structures of Compounds Designed to Probe the Interaction of NU2058 with CDKs

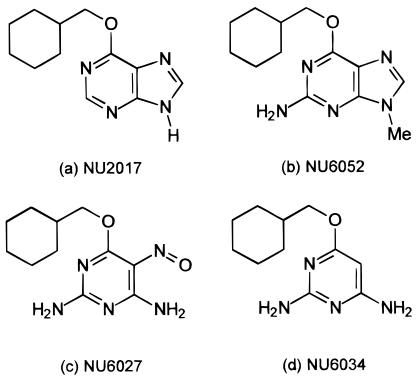

flavopiridol, consistent with preclinical in vivo data,[11,12] and Phase II trials are underway. However, enzyme inhibition studies have shown that the CDK specificity of flavopiridol is limited, CDKs 1, 2, and 4 being equally sensitive to inhibition by the compound.[8,13] Consistent with the lack of CDK specificity, whole cell studies have shown that following treatment with flavopiridol cell cycle arrest can occur at either the G1/S and/or G2/M checkpoints.[13−16]

In the search for more specific CDK inhibitors a number of pharmacophores have been investigated, prominent among which are the 6-aminopurine-based inhibitors.[17−24] Where studied, the 6-aminopurines have been shown to be competitive inhibitors with respect to ATP, and structural investigations with monomeric CDK2 have shown that certain of the compounds (e.g., olomoucine, roscovitine, and purvalanol B (Chart 1b−d, respectively) bind as expected in the ATP binding site.[21,25,26] However, the 6-aminopurines do not reproduce the hydrogen-bonding characteristics of ATP. Specifically, ATP forms a single hydrogen bond with Leu 83 of CDK2 through the N-1 position of the purine ring, and a second bond to Glu 81 through the N-6 position. In contrast, the 6-aminopurines interact with Leu 83 through the N-7 and N-6 positions, and Glu 81 via C-8.[21,25,26]

As part of a screening exercise, a series of guanine analogues were evaluated for their ability to inhibit CDK1. Surprisingly, given the lack of an exocyclic C-6 amino group and hence the potential for interaction with Leu 83 via this position, certain O^6-alkylguanines were found to be CDK1 inhibitors (L. Meijer, personal communication). This paper describes the inhibition of CDKs 1 and 2 by selected O^6-cyclohexylmethylguanines. The tumor cell growth inhibitory properties of O^6-cyclohexylmethylguanines and O^4-cyclohexylmethylpyrimidines designed to probe hydrogen bond interactions within the CDK2 active site, identified by crystal structure analysis, have also been determined.

Materials and Methods

Chemistry. O^6-Cyclohexylmethylguanine (NU2058, Chart 1e) was synthesized as previously reported,[27,28] using either 2-amino-6-chloropurine or 2-amino-6-(1,4-diazabicyclo[2.2.2]-oct-1-yl)purinium chloride as starting materials, respectively. The latter method has the advantage of easier purification of products and was also used to prepare O^6-cyclohexylmethylpurine (NU2017, Chart 2a). O^6-Cyclohexylmethyl-N^9-methylguanine (NU6052, Chart 2b) was synthesized from 2-amino-6-chloro-9-methylpurine, which was prepared by methylation of 2-amino-6-chloropurine. 2,6-Diamino-4-cyclohexylmethoxy-5-nitrosopyrimidine (NU6027, Chart 2c) and 2,6-diamino-4-cyclohexylmethoxypyrimidine (NU6034, Chart 2d) were synthesized from 2,6-diamino-4-chloropyrimidine as described previously.[29]

Experimental: NU2058. Cyclohexylmethanol (9.71 mmol) and sodium hydride (3.54 mmol) were stirred in anhydrous DMSO (8.0 mL) for 1 h, before addition of 2-amino-6-(1,4-diazabicyclo[2.2.2]oct-1-yl)purinium chloride (1.78 mmol). After the reaction was stirred for 48 h, glacial acetic acid was added to adjust the pH to 7. The solvent was removed, and the crude product was loaded onto a silica column, which was eluted with 10% MeOH/DCM. The desired product was obtained as a white solid (51%), mp 202−204 °C; λ_{max} (CH_3OH)/nm 281; IR 3350, 3200, 2900, 1640 cm^{-1}; ^1H NMR δ 1.5 (m, 11H, C_6H_{11}), 4.5 (d, 2H, OCH_2), 6.31 (s, 2H, NH_2), 7.92 (s, 1H, C^8H); ^{13}C NMR δ 25.5 (C4′), 26.3 (C3′ and C5′), 29.5 (C2′ and C6′), 37.2 (C1′), 70.8 (OCH_2), 137.9 (C8), 157.0 (C4), 160.1 (C2), 162.0 (C6); HRMS (EI) m/z 247 [M^+], 170, 151, 134, 109, 81. Anal. ($C_{12}H_{17}N_5O$) C, H, N.

NU2017. Cyclohexylmethanol (0.8 mL, 6.5 mmol) and sodium hydride (0.08 g, 3.33 mmol) were added to anhydrous DMSO (8.0 mL) under N_2, and the mixture was stirred for 1 h at room temperature. 6-(1,4-Diazabicyclo[2.2.2]octyl)purinium chloride (0.3 g, 1.13 mmol) was added, and stirring was continued for 3 days. The reaction was neutralized by addition of glacial acetic acid, and solvents were removed. Purification by column chromatography (eluent 10% MeOH/DCM) yielded a white solid (57%), mp 210−211 °C; ^1H NMR δ 1.25 (m, 5H, C_6H_{11}), 1.9 (m, 6H, C_6H_{11}), 4.4 (d, 2H, J = 6 Hz, OCH_2), 8.5 (s, 1H, C^2H or C^8H), 8.6 (s, 1H, C^2H or C^8H); HRMS (EI) m/z 232 (M^+), 149, 135, 119, 81, 41. Anal. ($C_{12}H_{16}N_4O$) C, H, N.

NU6052. 2-Amino-6-chloropurine (2.95 mmol) and potassium carbonate (2.95 mmol) in DMF (2 mL) were stirred vigorously for 30 min. Methyl iodide (3.25 mmol) was added, and stirring continued at room temperature for 18 h. The solvent was removed under reduced pressure. Purification by column chromatography (eluent 10% MeOH/DCM) yielded the N^9 isomer (62%, white solid, mp > 300 °C) as the predominant product. UV λ_{max} 247, 311 nm (MeOH); IR 3412, 3332, 3210, 2990, 1647, 1607, 1562 cm^{-1}; ^1H NMR δ 8.2 (s, 1H, C^8H), 7.0 (s, 2H, NH_2), 3.8 (s, 3H, CH_3); HRMS (EI) m/z 183.030693 [M^+ calc for $C_6H_6N_5Cl$], 148. Sodium (2.46 mmol) was added to cyclohexylmethanol (2 mL) at 90 °C. After 1 h, 2-amino-6-chloro-9-methylpurine (0.82 mmol) was added, and the reaction was stirred for a further 2 h. The reaction mixture was cooled to room temperature, after which the pH was adjusted to 7 by addition. The solvent was removed and the residue extracted with water (100 mL) and EtOAc (2 × 100 mL). The organic layers were combined, dried, and evaporated. The residue was purified by column chromatography (eluent 3% MeOH/DCM). Recrystallization from ethyl acetate/petrol yielded a white solid product (60%), mp 174−175 °C. UV λ_{max} 250, 283 nm (MeOH); IR 3382, 3338, 2922, 2850, 1651, 1607, 1582 cm^{-1}; ^1H NMR δ 1.0−1.5 and 1.7−2.0 (m, 11H, C_6H_{11}), 3.7 (s, 3H, CH_3), 4.3 (s, 2H, OCH_2), 6.5 (s, 2H, NH_2), 7.9 (s, 1H, H_8); HRMS (EI) m/z 261.157974 [M^+ calcd for $C_{13}H_{19}N_5O$ 261.158960], 178, 165, 148. Anal. ($C_{13}H_{19}N_5O$) C, H, N.

NU6034. Cyclohexylmethanol (30 mL) and sodium (32 mmol) were heated under N_2 at 150 °C for 90 min. 4-Chloro-2,6-diaminopyrimidine (30 mmol) was added, and the reaction mixture was refluxed at 180 °C for 2 h. The excess of cyclohexylmethanol was removed, and the residue was purified by column chromatography (eluent 10% MeOH/DCM). The product was recrystallized from MeOH yielding a white solid (70%), mp 142 °C; ^1H NMR δ 1.05 (m, 5H,), 1.85 (m, 6H), 4.0 (d, 2H, OCH_2), 5.15 (s, 1H, C^5H), 5.95 (s, 2H, NH_2), 6.1 (s, 2H, NH_2); HRMS (EI) m/z 222 [M^+]. Anal. ($C_{11}H_{18}N_4O$) C, H, N.

NU6027. 2,6-Diamino-4-cyclohexylmethoxypyrimidine (1.26 mmol) was dissolved in warm 30% glacial acetic acid solution (10 mL). The solution was heated to 80 °C, and aqueous sodium nitrite solution (1.72 mmol in 5 mL of H_2O) was added dropwise over 1 h. The reaction mixture was allowed to cool

to room temperature, and the violet crystals were filtered off and washed well with water. The crude product was purified by recrystallization from EtOH (83%), mp 254 °C; ^{1}H NMR δ 1.25 (m, 5H,), 2.0 (m, 6H), 4.4 (d, 2H, OCH_2), 7.9 (s, 2H, NH_2), 8.1 (s, 1H, N*H*), 10.2 (s, 1H, N*H*); HRMS (EI) *m*/*z* 251 [M$^+$]. Anal. ($C_{11}H_{17}N_5O_2$) C, H, N.

Enzyme Inhibition Studies. Inhibition of cyclin B1/CDK1 was assayed as previously described[17] using enzyme prepared from starfish oocytes (*Marthasterias glacialis*). Inhibition of cyclinA3/CDK2 was determined using a similar assay and an assay buffer comprised of 50 mM Tris-HCl pH 7.5 containing 5 mM $MgCl_2$. Cyclin A3/CDK2 was prepared as previously described[30] (cyclin A3 is a C-terminal cyclin A fragment encoding residues 171−432). The final ATP concentration in both CDK assays was 12.5 μM ,and the IC_{50} concentration for each compound is the concentration required to inhibit enzyme activity by 50% under the assay conditions used. To determine the K_m for ATP for cyclin B1/CDK1 and cyclin A3/CDK2, and K_i values for NU2058 and NU6027, assays were performed in the absence of inhibitor and at two fixed inhibitor concentrations (NU2058, 25 and 50 μM; NU6027, 5 and 10 μM), with ATP concentrations ranging from 6.25 to 800 μM. Data were fitted to the Michaelis−Menten equation using unweighted nonlinear least squares regression.

Expression, Purification, and Crystallization of Human CDK2. Human CDK2 was expressed in Sf9 insect cells using a recombinant baculovirus encoding CDK2 and purified following slight modifications to a published method.[30] Monomeric unphosphorylated CDK2 crystals were grown as previously described.[31]

X-ray Crystallography Data Collection and Processing. The CDK2/NU2058 data set was collected from a crystal soaked for 48 h in 5 mM NU2058 in 1× mother liquor solution (50 mM ammonium acetate, 10% PEG 3350, 15 mM NaCl, 100 mM HEPES, pH 7.4) plus 5% DMSO. The CDK2/NU6027 soak conditions were 26 h in 5mM NU6027 in 1x mother liquor solution plus 5% DMSO. CDK2/NU2017 soak conditions were similar. Data for the CDK2/NU2058 complex was collected on beamline 9.5, SRS, Daresbury, U.K. The CDK2/NU6027 complex data set was collected on X-RAY DIFFRACTION at the Elettra Light source, and the CDK2/NU2017 data set was collected on BM14 at the ESRF. In each case data were collected at 100 K after crystals had been transferred briefly to cryoprotectant (mother liquor containing 20% glycerol). Images were integrated with the DENZO package and subsequently scaled and merged using SCALEPACK.[32] Statistics for the CDK2/NU2058 and CDK2/NU6027 data sets are given in Table 1.

Structure Solution and Refinement. The starting model for the structure solution and refinement of the CDK2/inhibitor complexes was the CDK2/ATP structure, PDB code 1HCK.[25] This model included protein residues 1−36 and 41−298. Refinement of the structure was begun by carrying out rigid body refinement using REFMAC,[36] using sequentially higher resolution data. As the resolution of the data included was increased from 3.0 Å to approximately 2.0 Å, an increasing number of rigid bodies were used, so that initially the whole molecule was treated as a single rigid body, and finally five-residue segments were allowed to refine independently. Following rigid body refinement, the ($F_o - F_c$)αcalc maps included readily interpretable electron density for the bound inhibitors. Clear electron density also defined those residues involved in interactions with the inhibitors. The structure was then compared with $2F_o - F_c$ electron density maps using the program "O",[33] and minor structural changes were introduced. Following the first round of model building, a model of the appropriate ligand generated within SYBYL[34] was built into the electron density map and included in subsequent refinement steps. Appropriate parameters for the geometric restraints in subsequent refinement by the program REFMAC were taken from the SYBYL minimized structure. Refinement was then pursued with alternating cycles of interactive model building and maximum likelihood refinement using the program REFMAC.[35,36] Toward the end of the refinement, water molecules were added with ARP.[36,37] Statistics for the final models are given in Table 1 and the atomic coordinates are available in PDB files 1E1V (CDK2/NU2058) and 1E1X (CDK2/NU6027).

Table 1. Statistics of the Data Sets Used and of the Refined Structures

	CDK2/NU2058	CDK2/NU6027
cell dimensions (Å)	52.62, 71.05, 71.50	52.65, 69.90, 71.61
maximal resolution (Å)	1.95	1.85
observations	42 243	62 274
unique reflections, completeness (%)	17 940 (88.8)	22 399 (96.4)
R_{merge}[a]	0.065	0.057
mean $I/(I)$	12.3	16.3
highest resolution bin (Å)	2.04−1.95	1.93−1.85
completeness (%)	84.3	97.2
mean I/mean (I)	2.6	2.27
R_{merge}	0.313	0.372
protein atoms	2338	2338
residues	290	290
other atoms	174 water 18 NU2058	144 water 18 NU6027
resolution range (Å)	20.00−1.8	20.00−1.85
R_{conv}[b]	19.5	21.3
R_{free}[c]	26.9	28.1
mean main chain protein temperature factors (Å)^2	25.2	35.9
mean ligand temperature factors (Å)^2	16.9	42.6

[a] $R_{merge} = \sum_h\sum_j|I_{h,j} - \bar{I}_h|/\sum_h\sum_j|I_{h,j}|$ where $I_{h,j}$ is the intensity of the jth observation of unique reflection h. [b] $R_{conv} = \sum_h||F_{o_h}| - |F_{c_h}||/\sum_h|F_{o_h}|$ where F_{o_h} and F_{c_h} are the observed and calculated structure factor amplitudes for reflection h. [c] R_{free} is equivalent to R_{conv} but is calculated using a 5% disjoint set of reflections excluded from the least squares refinement stages.

Table 2. Inhibition of CDK1 and CDK2 and Cell Growth by Cyclohexylmethyl Guanine and Pyrimidine Derivatives

compound[a]	CDK1 inhibition K_i or IC_{50} (μM)[b]	CDK2 inhibition K_i or IC_{50} (μM)[b]	mean GI_{50} (μM)[c]
NU2058	$K_i = 5 \pm 1$	$K_i = 12 \pm 3$	13 ± 7
NU2017	$IC_{50} = 18 \pm 7$	$IC_{50} = 13(10-16)$	55
NU6052	$IC_{50} > 100$	$IC_{50} > 100$	>100
NU6027	$K_i = 2.5 \pm 0.4$	$K_i = 1.3 \pm 0.2$	10 ± 6
NU6034	$IC_{50} > 10$[d]	$IC_{50} > 10$[d]	>100

[a] For structures, see Charts 1 and 2. [b] IC_{50} is the concentration of inhibitor required to inhibit enzyme activity by 50% under the assay conditions used, and K_i is the associated inhibition constant. Values are from independent studies or the mean ± SD where $n = >3$ experiments or the mean and range for $n = 2$. [c] The mean GI_{50} is the mean of the concentrations of the compound required to inhibit cell growth by 50% in each of the cell lines (total = 57), mean ± SD where $n = >2$ experiments. [d] Less than 10% inhibition at 10 μM, the maximum achievable concentration.

Cell Growth Inhibition Studies. The growth inhibitory activity of the compounds was evaluated in the NCI in vitro cell line panel using the standard 48 h exposure assay and inhibitor concentrations ranging from 10^{-9} to 10^{-4} M.[38] Relationships between the profile of cell growth inhibition produced by the novel CDK inhibitors and that of standard anticancer agents, and the established CDK inhibitors olomoucine and flavopiridol, was investigated using the COMPARE algorithm.[39]

Results and Discussion

The lead guanine-based CDK inhibitor O^6-cyclohexylmethylguanine (NU2058, Chart 1e) was found to be an inhibitor of both CDK1 and CDK2 (Table 2). Enzyme kinetic studies demonstrated that the K_m for ATP for both CDK1 and CDK2 under the assay conditions used was 50 μM (51 ± 5 μM and 53 ± 6 μM,

respectively, mean ± SD, $n = 4$), and the K_i values for NU2058 were as follows: CDK1, 5 ± 1 μM; CDK2, 12 ± 3 μM (mean ± SD, $n = 4$). Against both enzymes, inhibition by NU2058 was competitive with respect to ATP.

Inhibitors were soaked into crystals of monomeric, unphosphorylated, CDK2 and the structures refined to the resolutions given in Table 1. The structure of CDK2 represents the minimal catalytic kinase core, constituted by two domains: a smaller N-terminal domain of approximately 80 residues formed principally from β-sheet, and a larger (~210 residue) predominantly α-helical C-terminal domain. The first complex characterized was CDK2/NU2058. Consistent with the enzyme inhibition data, NU2058 was found to bind within the ATP site of CDK2. A comparison of the refined structure to that of apo-CDK2,[40] and to other CDK2-inhibitor complexes,[21,25,26,31,41,42] revealed that NU2058 employs a number of novel interactions to bind to CDK2. Figure 1 shows the site of binding of NU2058 to CDK2 and the hydrogen-bonding pattern between NU2058 and the CDK2 backbone.

As shown in Figure 1b, N-9 of NU2058 donates a hydrogen bond to the peptide oxygen of Glu 81, the NH group of Leu 83 donates a hydrogen bond to NU2058 N-3, and 2-NH_2 acts as a donor to the carbonyl group of Leu 83. Although residues 80−84 constitute part of the hinge between the N- and C-terminal domains of CDK2, the interactions do not result in a significant change in relative domain orientation. Importantly, NU2058 binds into the ATP binding site cleft in a different orientation from that of the purines olomoucine, roscovitine, or purvalanol B (Figure 2).[21,25,26] The hydrogen bonds to the carbonyl group of Glu 81, and the amide group of Leu 83, are also made by isopentenyladenine and ATP, while the hydrogen bond with the carbonyl group of Leu 83 is also seen in the complexes of CDK2 with olomoucine, roscovitine, and purvalanol B. Hydrogen bonds to these amino acids are also observed with members of the indirubin class of CDK2 inhibitors,[42] although these are structurally dissimilar from NU2058. The binding of the guanine ring of NU2058 is not coplanar with that of the ATP adenine ring in the CDK2/ATP structure,[25] and minor variations in ring position are observed among the inhibitors described here. The cyclohexylmethyl group at the O^6-position of NU2058 occupies space close to where the ribose ring of ATP binds, although it cannot mimic the hydrogen-bonding interactions of the ribose 2′- and 3′-hydroxyls.

In the apo-CDK2 structure, and in other monomeric CDK2-inhibitor complex structures, two regions of CDK2 have been reported to be flexible.[25,31,40] The missing residues constitute the loop connecting strand β3 to helix αC, and the "activation segment" containing Thr 160 which is phosphorylated in the fully active CDK2-cyclin A complex.[43] NU2058 binding to CDK2 is accompanied by a marked decrease in the main chain temperature factors for all residues, but it is particularly noticeable for residues in strand β1 and the activation loop and results in a readily interpretable electron density map for both these regions (Figure 3a). Additional interactions between the NU2058 O^6-substituent and the glycine-rich loop accompany stabilization of the

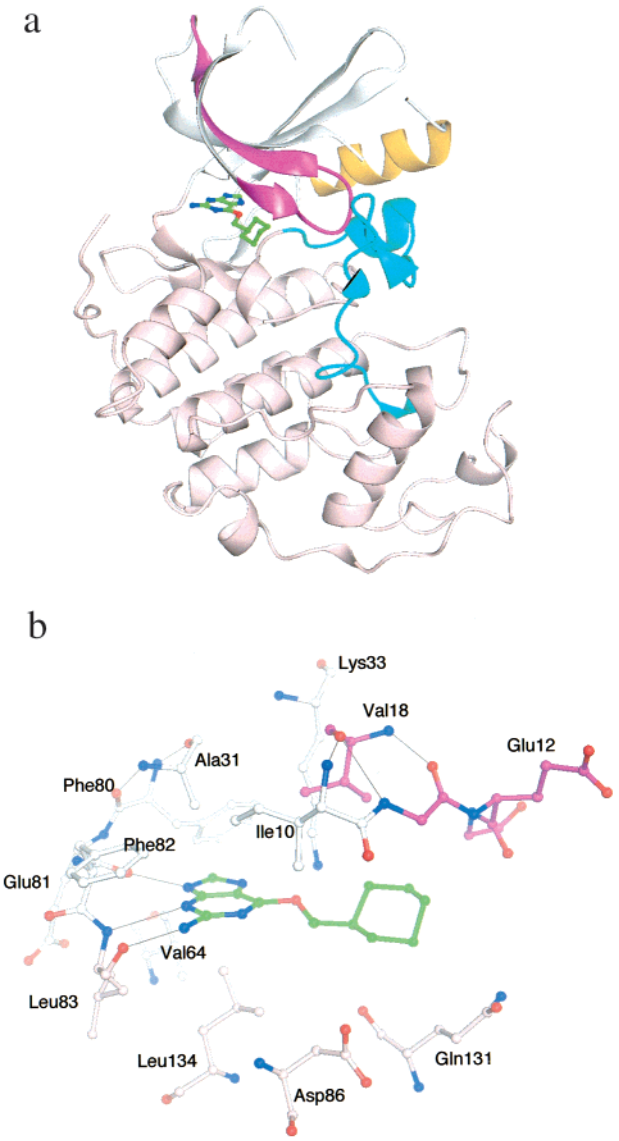

Figure 1. Interaction of NU2058 with monomeric CDK2: (a) NU2058 binding to CDK2 in the ATP binding site cleft. The structure is shown in a cartoon representation. The N-terminal domain (residues 1−82) is colored white, with the exceptions of the glycine-rich loop (residues 11−24) colored magenta, and the C-helix (PSTAIRE helix, residues 46−55) colored gold. The chain is broken at residues 36−43 for which there is no electron density in the maps. NU2058 is shown in ball-and-stick representation at the interface between the N- and C-terminal domains. The C-terminal domain is colored pink, with the activation segment (residues 145−172) highlighted in cyan. (b) Schematic drawing of NU2058 bound to CDK2. Conserved hydrogen bonds between the CDK2 backbone at residues Glu 81 and Leu 83 and NU2058 are illustrated by thin lines. CDK2 residues within 4 Å of the ligand are drawn with carbon atoms colored as for Figure 1a. Selected CDK2 residues are labeled.

activation loop (Figure 3a). These interactions are predominantly hydrophobic between the cyclohexyl group and a hydrophobic patch on the glycine loop contributed by the side chains of residues Val 18 and the peptide backbone around residue Gly 11 (Figure 3c). Residues in the activation loop do not interact directly with NU2058. The activation segment conformation is similar to that first reported by DeBondt et al.,[40] for the structure of the monomeric CDK2/ATP complex. Ordering of both the glycine-rich loop and the activation

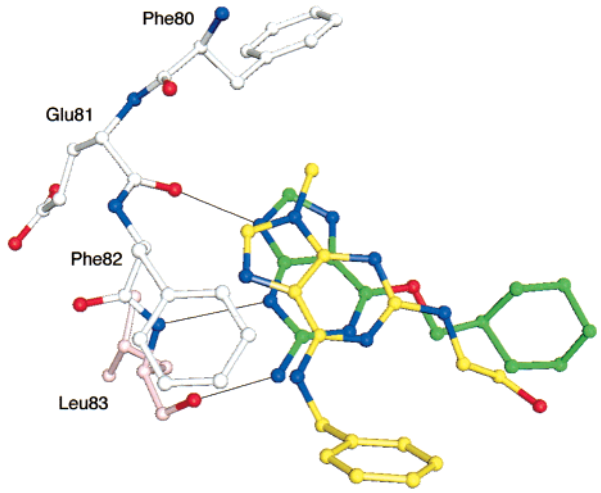

Figure 2. Overlay of the CDK2/olomoucine structure with that of the CDK2/NU2058 complex in the vicinities of the inhibitor binding sites. Conserved hydrogen bonds between the CDK2 backbone, at residues Glu 81 and Leu 83, and NU2058 are drawn as thin lines. Only CDK2 residues Phe 80 to Leu 83 in the CDK2/NU2058 structure are included for clarity. CDK2 carbon atoms are colored as for Figure 1a; NU2058 carbon atoms are green, and olomoucine carbon atoms are yellow. The O^6-cyclohexyl substituent of NU2058 and the 2-hydroxyethyl group of olomoucine occupy the ATP ribose binding site. The olomoucine N^6-group binds outside the ATP cleft. Roscovitine and purvalanol B bind to CDK2 in the same orientation as olomoucine.

segment is not observed in all guanine- and pyrimidine-based CDK2/inhibitor complex structures (results not shown). For example, binding of NU6027 to CDK2 does not result in ordering of these regions (Figure 3b).

On the basis of the structure shown in Figure 1, two additional O^6-cyclohexylmethylguanine derivatives were prepared in order to determine the relative importance of the hydrogen bonds at the 2-NH_2 and N-9 positions of NU2058. These were O^6-cyclohexylmethylpurine (NU2017, Chart 2a) and O^6-cyclohexylmethyl-N^9-methylguanine (NU6052, Chart 2b). As shown in Table 2, both compounds were less active than NU2058 as inhibitors of CDK1 and/or CDK2, implying that the hydrogen bonds formed by the 2-NH_2 and N-9 functions of NU2058 can both contribute to the potency of the molecule. Of the two NU2058 derivatives NU2017 retained activity, particularly against CDK2, indicating that the hydrogen bond formed by the 2-NH_2 is not indispensable. The CDK2/NU2017 structure confirmed that NU2017 binds to CDK2 within the ATP binding site in the same orientation as NU2058 (data not shown).

In an attempt to reproduce the triplet of hydrogen bonds observed for NU2058 (Figure 1b) in a molecule lacking the purine nucleus, the pyrimidine NU6027 (2,6-diamino-O^4-cyclohexylmethyloxy-5-nitrosopyrimidine, Chart 2c) was prepared. In designing NU6027, note was taken of the need to maintain the 6-amino group (equivalent to N-9 in NU2058) in the correct orientation to enable hydrogen bonding with the peptide oxygen of Glu-81. To do so, a nitroso group was introduced at the 5-position in the expectation that the 5-nitroso group would form an intramolecular hydrogen bond with the 6-amino group, thereby establishing the correct geometry for the remaining hydrogen atom on the 6-NH_2 group. As shown in Table 2, NU6027 was indeed a potent inhibitor of both CDK1 and CDK2, with K_i values of 2.5 ± 0.4 μM and 1.3 ± 0.2 μM, respectively (mean ± SD, n = 4). As in the case of NU2058, the pyrimidine NU6027 was a competitive inhibitor of both CDK1 and CDK2 with respect to ATP.

NU6027 was soaked into crystals of monomeric CDK2 and the structure refined to a resolution of 1.85 Å. As shown in Figure 4, as anticipated, the 6-NH_2 group of NU6027 donates a hydrogen bond to the peptide oxygen of Glu 81, the NH group of Leu 83 donates a hydrogen bond to N-1, and the NH_2 group attached to C-2 acts as a donor to the carbonyl group of Leu 83. Importantly, the predicted intramolecular hydrogen bond between the 5-nitroso and 6-NH_2 groups of NU6027 was observed, and this interaction was apparently the only contribution to binding made by the 5-nitroso group. To confirm the importance of the intramolecular hydrogen bond between the 5- and 6-substituents of NU6027, the derivative lacking the 5-nitroso group was synthesized (2,6-diamino-O^4-cyclohexylmethyloxypyrimidine, NU6034, Chart 2d). As shown in Table 2, NU6034 did not inhibit CDK1 or -2 at the concentrations tested, suggesting that the intramolecular hydrogen bond between the 5- and 6-substituents of NU6027, and hence the correct orientation of the 6-NH_2 group, is required for activity.

Having defined the unique interactions of the novel guanine- and pyrimidine-based CDK inhibitors with CDK2, the effects of the compounds on the growth of human tumor cells was investigated. Fifty-seven of the cell lines in the National Cancer Institute in vitro cell line panel were used for these studies in order to allow comparisons with other compounds, both standard anticancer agents and known CDK inhibitors. Table 2 shows the mean GI_{50} data (concentrations required to inhibit cell growth by 50% over 48 h) for the compounds investigated as CDK inhibitors. In the purine series, NU2058 was the most potent compound with a mean GI_{50} value of 13 ± 7 μM. The compound lacking the 2-NH_2 substituent (NU2017, Chart 2a) was less potent than NU2058, a result consistent with the reduced activity of the compound as a CDK1 inhibitor (Table 2). The N-9 methyl derivative of NU2058 (NU6052, Chart 2b), which cannot by definition form a purine N-9 to Glu 81 hydrogen bond and did not inhibit CDK1 or -2 in the isolated enzyme assays, was not an inhibitor of cell growth in most of the cell lines (GI_{50} > 100 μM in 50/57 cell lines studied). Similar in vitro growth inhibition studies were performed with the pyrimidines NU6027 (Chart 2c) and NU6034 (Chart 2d). NU6027 was growth inhibitory with mean GI_{50} values of 10 ± 6 μM whereas NU6034, which cannot form an intramolecular hydrogen bond in order to orientate correctly the 6-NH_2 substituent, was not growth inhibitory (GI_{50} > 100 μM in 49/57 cell lines studied).

A COMPARE analysis was performed against the standard anticancer agent database for both NU2058 and NU6027. Neither compound generated Pearson correlation coefficients of >0.5 for the GI_{50} COMPARE analysis, and hence these CDK inhibitors have a pattern of cellular activity distinct from that of known classes of antitumor agents. Interestingly, the COMPARE analysis for the relationship between the GI_{50} sensitivity profiles of NU2058 and NU6027 versus flavopiridol and

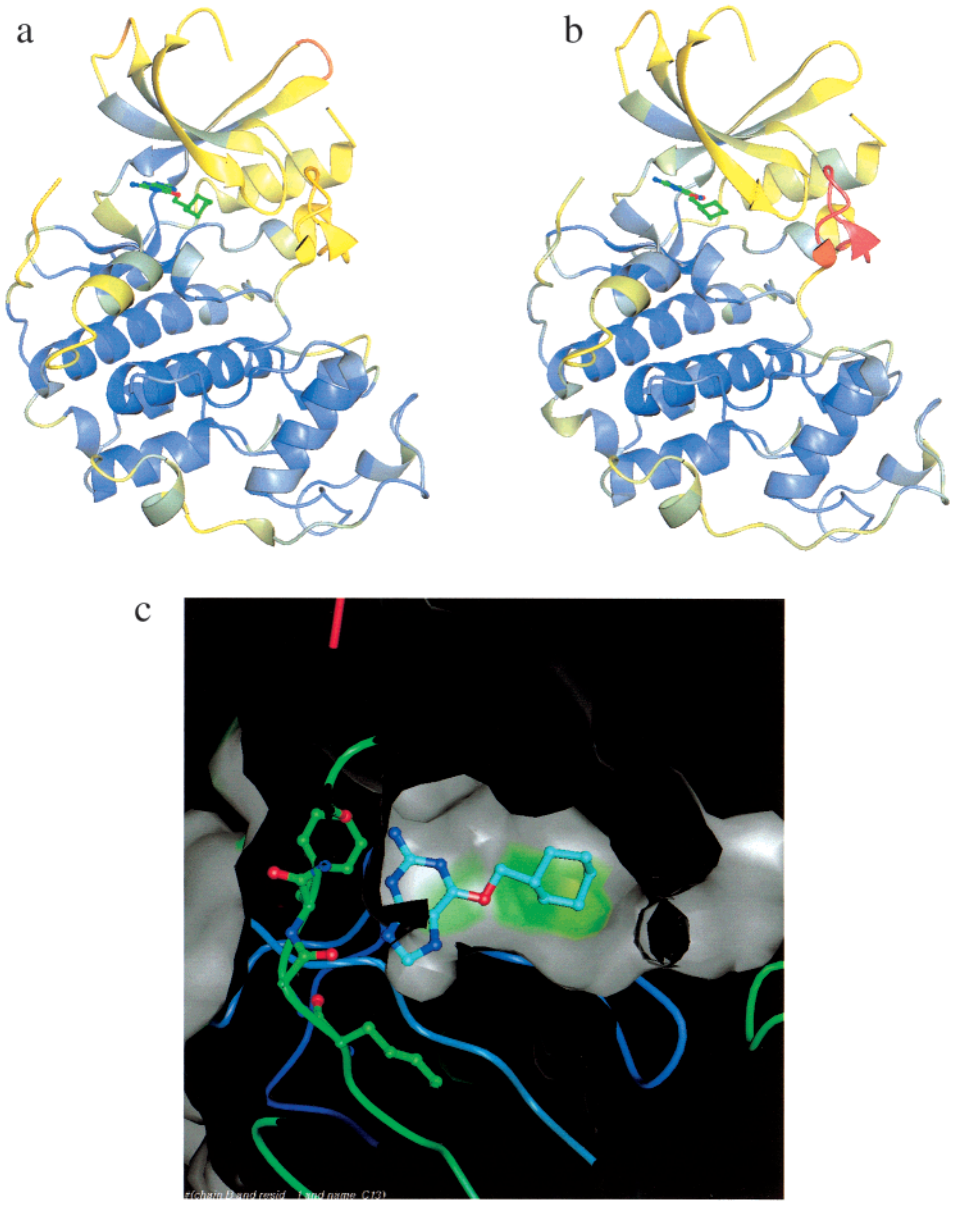

Figure 3. (a, b) Ribbon diagrams of CDK2/inhibitor complexes colored by temperature factor such that deep blue corresponds to a temperature factor at least 10 Å^2 less than the average main chain B-factor and deep red corresponds to a temperature factor greater than or equal to 40 Å^2 greater than the average main chain B-factor. The inhibitors are shown in ball-and-stick representation. (a) CDK2/NU2058 complex, (b) CDK2/NU6027 complex. (c) The shape and surface properties of the CDK2 ATP binding site cleft as seen in complex with NU2058. The Connolly molecular surface of CDK2 is rendered looking onto the N-terminal domain at the surface of the glycine-loop sequence to show the hydrophobic region that interacts with the NU2058 O^6-cyclohexyl group.[45] The surface is colored such that regions showing a preference for hydrophobic interactions (as calculated by the program GRID[46]) range from yellow (strong preference) to gray (no particular preference). A hydrophobic patch generated by the side chain of Val 18 and the peptide backbone around Gly 11 is apparent.

olomoucine also yielded low Pearson correlation coefficients, i.e., 0.22−0.38. These low values are in contrast to the value for the relationship between flavopiridol and olomoucine (0.57), and NU2058 and NU6027 (0.65). Together with the enzyme inhibition and structural studies, these in vitro chemosensitivity data suggest that the distinct mode of binding of NU2058 and NU6027 to CDKs has direct consequences in terms of cell growth inhibition and differential activity with respect to other CDK inhibitors.

The CDKs are prominent among novel targets for cancer therapy because of the frequency of abnormalities in genes which encode proteins that either directly (e.g., p 16, cyclin D) or indirectly (e.g., p 53) control CDKs or are CDK substrates (e.g., retinoblastoma protein). Preclinical[11,12] and more recently clinical[10] studies with the prototype CDK inhibitor flavopiridol have shown that CDK inhibitors can have single agent antitumor activity, and initial combination studies with cytotoxic drugs are encouraging.[44]

The first generation of CDK inhibitors, exemplified by flavopiridol and olomoucine, have either limited specificity for individual CDKs (flavopiridol[13]) or relatively poor potency as inhibitors of the CDK enzymes and tumor cell growth (olomoucine[17,18]). Hence a number of groups have initiated analogue development programs focused largely on the 6-aminopurine pharmacophore.[17−24] These latter studies have shown that it

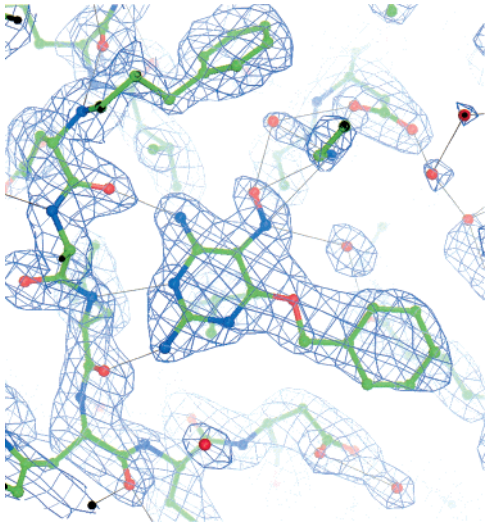

Figure 4. NU6027 bound to CDK2. Conserved hydrogen bonds between the CDK2 backbone at residues Glu 81 and Leu 83 and NU6027 are illustrated by thin lines. The $(2F_o - F_c)\alpha$calc electron density for the CDK/NU6027 complex included in the figure was calculated at the end of the refinement ($R_{conv} = 21.3\%$, $R_{free} = 28.1\%$) using map coefficients output from REFMAC with resolution between 20.0 and 1.85 Å. The map is contoured at a level of 0.3 eÅ^{-3}, corresponding to 1.1 times the root-mean-square deviation of the map from the mean value. The intramolecular bond between the 5-nitroso group and the 6-amino group establishes the correct geometry for the 6-amino group to act as a hydrogen bond donor to the backbone oxygen atom of Glu 81.

is possible to develop CDK inhibitors with nanomolar potency as CDK inhibitors and mean GI_{50} values in the NCI cell line screen, or IC_{50} values for other human tumor cell lines, in the low micromolar range. The challenge in the area of small molecule CDK inhibitor development is currently to identify compounds with improved specificity for individual CDKs, coupled with greater in vitro potency against tumor cell lines. To meet this challenge, additional CDK inhibitor pharmacophores would be valuable, and the current report describes the identification of the guanine pharmacophore and novel pyrimidine-based inhibitors derived from a knowledge of the binding of the guanine-based inhibitors to CDK2. The lead compounds in the two series (NU2058 and NU6027) display CDK inhibitory potency similar to that of olomoucine, which has IC_{50} values against cyclinB/CDK1 and cyclinA or E/CDK2 of 7 μM,[17] and activity against cell lines equivalent or superior to that of roscovitine (the mean GI_{50} of roscovitine in the NCI cell line screen is 16 μM[18]). These data suggest that NU2058 and NU6027 may be able to enter cells more readily than the 6-aminopurine-based inhibitors.

High-throughput cell line screening and protein structure-based drug design are two of the most important contemporary approaches to drug discovery. However, it can be difficult to show that effects in whole cells of chemical changes to inhibitors, introduced on the basis of information from inhibitor−protein structures, are in fact due to interactions with the intended target of the compound. The approach taken here was to synthesize compounds designed to delete what appeared, from the NU2058−CDK2 structure, to be critical hydrogen bond interactions, namely, the bonds between purine NH-9 to Glu 81 and purine 2-NH_2 to Leu 83. The inhibitors so produced had either reduced activity against CDK1 (NU2017) or no activity (NU6052) at the concentrations tested. Importantly, the same relative effects were seen in tumor cell growth inhibition studies, i.e., reduced activity with NU2017 and no activity with NU6052, suggesting that growth inhibition in the whole cell activity was indeed a reflection of kinase inhibition. Detailed studies of the cellular pharmacology of NU2058 and NU6027, in comparison to olomoucine, are currently ongoing. Preliminary studies in MCF7 cells have shown that, consistent with inhibition of both CDK1 and CDK2, treatment with NU2058 and NU6027 causes a reduction in the number of cells in S-phase but not G1 or G2/M (J. Bentley and C. Arris, unpublished results).

An important feature of protein structure-based drug design is the ability to predict novel pharmacophores once important sites for inhibitor−protein interactions have been identified. In the current study, identification of the triplet of hydrogen bonds formed between NU2058 and the ATP binding site of CDK2 led to the design of NU6027. Further detailed structure−activity studies based on both the guanine and pyrimidine pharmacophores are underway and will be described elsewhere.

Acknowledgment. The authors thank David Morgan for his generous gift of the *Ac*CDK2 baculovirus and Tim Hunt for the cyclin A3 expression construct. The staff at station 9.5, Daresbury, beamline BM14, ESRF, and X-RAY DIFFRACTION, Elettra, provided excellent facilities and advice during data collection. At the LMB the authors thank I. Taylor, R. Bryan, Y. Huang, K. Measures, and S. Lee. The authors are also grateful to Dr. Hans Hendriks of the New Drug Development Office (Amsterdam, The Netherlands) for coordinating the initial screening of compounds by Dr. Laurent Meijer and Ms. Sophie LeClerq (CNRS, Roscoff, France) to whom they are also indebted. The assistance of Ms. Susanne Radkte (NCI Liaison Office, Brussels) and Ms. Ronnie Verdon and Dr. Sally Burtles (CRC Drug Development Office, London, U.K) in facilitating the evaluation of compounds in the NCI cell line screen is also much appreciated. This research was supported by grants from the Cancer Research Campaign, The Royal Society, The Medical Research Council, and the BBSRC.

References

(1) Pines, J. Cyclins and cyclin-dependent kinases: A biochemical view. *Biochem. J.* **1995**, *308*, 697−711.
(2) Chevalier, S.; Blow, J. J. Cell cycle control of replication initiation in eukaryotes. *Curr. Opin. Cell Biol.* **1996**, *8*, 815−821.
(3) Nurse, P.; Masui, Y.; Hartwell, L. Understanding the cell cycle. *Nature Med.* **1998**, *4*, 1103−1106.
(4) Sherr, C. J. Cancer cell cycles. *Science* **1996**, *274*, 1672−1677.
(5) Morgan, D. O. Cyclin-dependent kinases: Engines, Clocks and Microprocessors. *Annu. Rev. Cell Dev. Biol.* **1997**, *13*, 261−291.
(6) Hall, M.; Peters, G. Genetics alterations of cyclins, cyclin-dependent dependent kinases, and Cdk inhibitors in human cancer. *Adv. Cancer Res.* **1996**, *68*, 67−108.
(7) Gray, N.; Detivaud, L.; Doerig, D.; Meijer, L. ATP-site inhibitors of cyclin-dependent kinases. *Curr. Med. Chem.* **1999**, *6*, 859−875.
(8) Walker, D. H. Small-molecule inhibitors of cyclin-dependent kinases: Molecular tools and potential therapeutics. *Curr. Top. Microbiol. Immunol.* **1998**, *227*, 149−165.
(9) Garrett, M. D.; Fattaey, A. CDK inhibition and cancer therapy. *Curr. Opin. Genet. Dev.* **1999**, *9*, 104−111.

(10) Senderowicz, A. M.; Headlee, D.; Stinson, S. F.; Lush, R. M.; Kalil, N.; Villalba, L.; Hill, K.; Steinberg, S. M.; Figg, W. D.; Tompkins, A.; Arbuck, S. G.; Sausville, E. A. Phase I trial of continuous infusion flavopiridol, a novel cyclin-dependent kinase inhibitor, in patients with refractory neoplasms. *J. Clin. Oncol.* **1998**, *16*, 2986−2999.
(11) Drees, M.; Dengler, W. A.; Roth, T.; Labonte, H.; Mayo, J.; Malspeis, L.; Grever, M.; Sausville, E. A.; Fiebig, H. H. Flavopiridol (L86-8275): Selective antitumour activity in vitro and activity in vivo for prostate carcinoma cells. *Clin. Cancer Res.* **1997**, *3*, 2273−279.
(12) Arguello, F.; Alexander, M.; Sterry, J. A.; Tudor, G.; Smith, E. M.; Kalavar, N. T.; Greene, J. F.; Koss, W.; Morgan, C. D.; Stinson, S. F.; Siford, T. J.; Alvord, W. G.; Klabansky, R. L.; Sausville, E. A. Flavopiridol induces apoptosis of normal lymphoid cells, causes immunosuppression, and has potent antitumour activity in vivo against human leukaemia and lymphoma xenografts. *Blood* **1998**, *91*, 2482−2490.
(13) Carlson, B. A.; Dunbay, M. M.; Sausville, E. A.; Brizuela, L.; Worland, P. J. Flavopiridol induces G_1 arrest with inhibition of cyclin-dependent kinase (CDK) 2 and CDK4 in human breast carcinoma cells. *Cancer Res.* **1996**, *56*, 2973−2978.
(14) Kaur, G.; Stetler-Stevenson, M.; Sebers, S.; Worland, P.; Sedlacek, H.; Myers, C.; Czech, J.; Naik, R.; Sausville, E. Growth inhibition with reversible cell cycle arrest of carcinoma cells by flavone L86-8275. *JNCI, J. Natl. Cancer Inst.***1992**, *84*, 1736−1740.
(15) Schrump, D. S.; Matthews, W.; Che, G. A.; Mixon, A.; Altorki, N. K. Flavopiridol mediates cell cycle arrest and apoptosis in esophageal cancer cells. *Clin. Cancer. Res.* **1998**, *4*, 2885−2890.
(16) Parker, B. W.; Kaur, G.; Nieves-Neira, W.; Taimi, M.; Kohlhagen, G.; Taimi, M.; Kohlhagen, G.; Shimizu, T.; Losiewicz, M. D.; Pommier, Y.; Sausville, E. A.; Senderowicz, A. M. Early induction of apoptosis in haematopoietic cell lines after exposure to flavopiridol. *Blood* **1998**, *91*, 458−465.
(17) Vesely, J.; Havlicek, L.; Strnad, M.; Blow, J. J.; Donella-Deana, A.; Pinna, L.; Letham, D. S.; Kato, J.-Y.; Detivaud, L.; Leclerc, S.; Meijer, L. Inhibition of cyclin-dependent kinases by purine analogues. *Eur. J. Biochem.* **1994**, *224*, 771−786.
(18) Meijer, L.; Borgne, A.; Mulner, O.; Chong, J. P. J.; Blow, J. J.; Inagaki, N.; Inagaki, M.; Delcros, J.-L.; Moulinoux, J.-P. Biochemical and cellular effects of roscovitine, a potent and selective inhibitor of cyclin-dependent kinases cdc2, cdk2 and cdk5. *Eur. J. Biochem.* **1997**, *243*, 527−536.
(19) Brooks, E. E.; Gray, N. S.; Joly, A.; Kerwar, S. S.; Lum, R.; Mackman, R. L.; Norma, T. C.; Rosete, J.; Rowe, M.; Schow, S. R.; Schultz, P. G.; Wang, X.; Wick, M. M.; Schiffman, D. CVT-313, a specific and potent inhibitor of CDK2 that prevents neointimal proliferation. *J. Biol. Chem.* **1997**, *272*, 29207−29211.
(20) Schow, S. R.; Mackman, R. L.; Blum, C. L.; Brooks, E.; Horsma, A. G.; Joly, A.; Kerwar, S. S.; Lee, G.; Schiffman, D.; Nelson, M. G.; Wang, X.; Wick, M. M.; Zhang, X.; Lum, R. T. Synthesis and activity of 2,6,9-trisubstituted purines. *Bioorg. Med. Chem. Lett.* **1997**, *7*, 2697−2702.
(21) Gray, N. S.; Wodicka, L.; Thunnissen, A.-M. W. H.; Norman, T. C.; Kwon, S.; Espinoza, F. H.; Morgan, D. O.; Barnes, G.; LeClerc, S.; Meijer, L.; Kim, S.-H.; Lockhart, D. J.; Schultz, P. G. Exploiting chemical libraries, structure, and genomics in the search for kinase inhibitors. *Science* **1998**, *281*, 533−538.
(22) LeGraverend, M.; Ludwig, O.; Bisagni, E.; LeClerc, S.; Meijer, L. Synthesis of C2 alkynylated purines, a new family of potent inhibitors of cyclin-dependent kinases. *Bioorg. Med. Chem. Lett.* **1998**, *8*, 793−798.
(23) Imbach, P.; Capraro, H.-G.; Furet, P.; Mett, H.; Meyer, T.; Zimmermann, J. 2,6,9-Trisubstituted purines: Optimization towards highly potent and selective CDK1 inhibitors. *Bioorg. Med. Chem. Lett.* **1999**, *9*, 91−96.
(24) Chang, Y.-T.; Gray, N. S.; Rosania, G. R.; Sutherlin, D. P.; Kwon, S.; Norman, T. C.; Sarohia, R.; Leost, M.; Meijer, M.; Schultz, P. G. Synthesis and application of functionally diverse 2,6,9-trisubstituted purine libraries as CDK inhibitors. *Chem. Biol.* **1999**, *6*, 361−375.
(25) Schulze-Gahmen, U.; Brandsen, J.; Jones, H. D.; Morgan, D. O.; Meijer, L.; Vesely, J.; Kim, S.-H. Multiple modes of ligand recognition: Crystal structure of cyclin-dependent protein kinase 2 in complex with ATP and two inhibitors, olomoucine and isopentenyladenine. *Proteins* **1995**, *22*, 378−391.
(26) de Azevedo, W. F., Jr.; LeClerc, S.; Meijer, L.; Havlicek, L.; Strnad, M.; Kim, S.-H. Inhibition of cyclin-dependent kinases by purine analogues. Crystal structure of human cdk2 complexed with roscovitine. *Eur. J. Biochem.* **1997**, *243*, 518−526.
(27) Arris, C. E.; Bleasdale, C.; Calvert, A. H.; Curtin, N. J.; Dalby, C.; Golding, B. T.; Griffin, R. J.; Lunn, J. M.; Major, G. N.; Newell, D. R. Probing the active site and mechanism of action of O^6-alkylguanine-DNA alkyltransferase with substrate analogues. *Anticancer Drug Design* **1994**, *9*, 401−408.
(28) Lembicz, N. K.; Grant, S.; Clegg, W.; Griffin, R. J.; Heath, S. L.; Golding, B. T. Facilitation of displacements at the 6-position of purines by the use of 1,4-diazabicyclo[2,2,2]octane as leaving group. *J. Chem. Soc., Perkin Trans. 1* **1997**, 185−186.
(29) Pfleiderer, W.; Lohrmann, R. Synthesis of 2-amino-4-alkoxypteridine. *Chem. Ber.* **1961**, *94*, 12−18.
(30) Brown, N. R.; Noble, M. E. M.; Lawrie, A. M.; Morris, M. C.; Tunnah, P.; Divita, G.; Johnson, L. N.; Endicott, J. A. Effects of phosphorylation of threonine 160 on CDK2 structure and activity. *J. Biol. Chem.* **1999**, *274*, 8746−8756.
(31) Lawrie, A. M.; Noble, M. E. M.; Tunnah, P.; Brown, N. R.; Johnson, L. N.; Endicott, J. A. Protein kinase inhibition by staurosporine: Details of the molecular interaction determined by the X-ray crystallographic analysis of a CDK2-staurosporine complex. *Nature Struct. Biol.* **1997**, *4*, 796−802.
(32) Otwinowski, Z. Oscillation data reduction program. In DL/SC1/R34; Sawyer, L., Isaacs, N., Bailey, S., Eds.; SERC Laboratory: Daresbury, Warrington, U.K., 1993; pp 56−62.
(33) Jones, T. A.; Zou, J. Y.; Cowan, S. W.; Kjeldgaard, M. Improved method for building models in electron density maps and the location of errors in these models. *Acta Crystallogr.* **1991**, *A47*, 110−119.
(34) *Sybyl Molecular Modelling Software*; Tripos Associates Inc.: St. Louis, MO, 1992.
(35) Murshudov, G. N.; Vagen, A. A.; Dodson, E. J. Refinement of macromolecular structures by the maximum-likelihood method. *Acta Crystallogr.* **1997**, *D53*, 240−255.
(36) Collaborative Computational Project, Number 4. The CCP4 suite: programs for protein crystallography. *Acta Crystallogr.* **1994**, *D50*, 760−763.
(37) Lamzin, V. S.; Wilson, K. S. Automated refinement of protein models. *Acta Crystallogr.* **1993**, *D49*, 129−147.
(38) Monks, A.; Scudiero, D.; Skehan, P.; Shoemaker, R.; Paull, K.; Vistica, D.; Hose, C.; Langley, J.; Cronise, P.; Vaigro-Wolff, A.; Gray-Goodrich, M.; Campbell, H.; Mayo, J.; Boyd, M. Feasibility of a high-flux anticancer drug screen using a diverse panel of cultured human tumor cell lines. *JNCI, J. Natl. Cancer Inst.* **1991**, *83*, 757−766.
(39) Paull, K. D.; Shoemaker, R. H.; Hodes, L.; Monks, A.; Scudiero, D. A.; Rubinstein, L.; Plowman, J.; Boyd, M. R. Display and analysis of differential activity of drugs against human tumor cell lines: Development of mean graph and COMPARE algorithm. *JNCI, J. Natl. Cancer Inst.* **1989**, *81*, 1088−1092.
(40) De Bondt, H. L.; Rosenblatt, J.; Jancarik, J.; Jones, H. D.; Morgan, D. O.; Kim, S.-H. Crystal structure of cyclin-dependent kinase 2. *Nature* **1993**, *363*, 595−602.
(41) de Azevedo, W., Jr.; Mueller-Dieckmann, H.-J.; Schulze-Gahmen, U.; Worland, P. J.; Sausville, E.; Kim, S.-H. Structural basis for specificity and potency of a flavonoid inhibitor of human CDK2, a cell cycle kinase. *Proc. Natl. Acad. Sci. U.S.A.* **1996**, *93*, 2735−2740.
(42) Hoessel, R.; Leclerc, S.; Endicott, J. A.; Noble, M. E. M.; Lawrie, A.; Tunnah, P.; Leost, M.; Damiens, E.; Marie, D.; Marko, D.; Niederberger, E.; Tang, W.; Eisenbrand, G.; Meijer, L. Indirubin, the active constituent of a Chinese antileukaemia medicine, inhibits cyclin-dependent kinases. *Nature Cell Biol.* **1999**, *1*, 60−67.
(43) Russo, A.; Jeffrey, P. D.; Pavletich, N. P. Structural basis of cyclin-dependent kinase activation by phosphorylation. *Nature Struct. Biol.* **1996**, *3*, 696−700.
(44) Ongkeko, W.; Ferguson, D. J. P.; Harris, A. L.; Norbury, C. Inactivation of Cdc2 increases the level of apoptosis induced by DNA damage. *J. Cell Sci.* **1995**, *108*, 2897−2904.
(45) Connolly, M. Molecular surface triangulation. *J. Appl. Crystallogr.* **1985**, *18*, 499−505.
(46) Goodford, P. Multivariate characterization of molecules for QSAR. *J. Chemom.* **1996**, *10*, 107−117.

JM990628O